Wageningen University

Master Thesis

CloudRoots: an Integrated Measurement and 0-D Modelling approach of Vegetation-Atmosphere Interactions

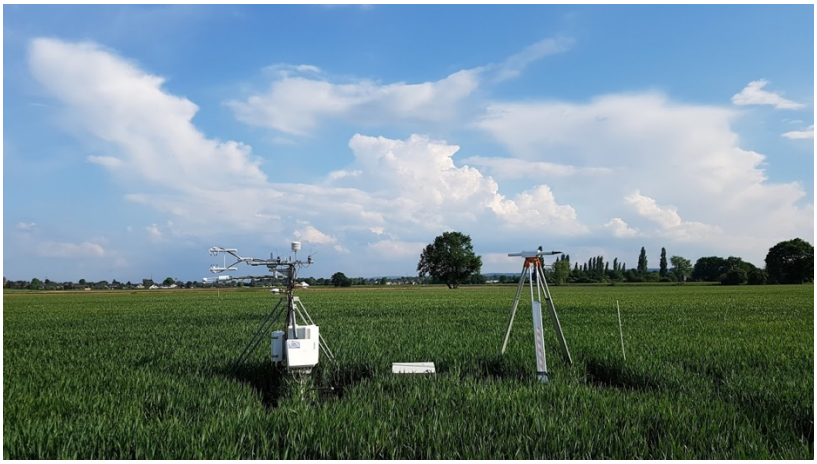

Gabriela Miranda García

Supervisor: dr.ir. Oscar Hartogensis
Examiner: prof.dr. Jordi Vilà-Guerau de Arellano

20/04/2019

Wageningen University

Abstract

CloudRoots: an Integrated Measurement and 0-D Modelling approach of Vegetation-Atmosphere Interactions

by Gabriela Miranda García

The challenge in the representation of the vegetation-atmosphere system is to connect different scales at which the transport of moisture and heat take place in a heterogeneous landscape. The purpose of this study is to connect processes at leaf-field scale to field-boundary layer scale using the 0-D mixed-layer model CLASS over a heterogeneous lanscape. To do this, we used the observations from CloudRoots, a campaign performed in Selhausen, Germany over a wheat crop. The data collection was at leaf, field and boundary layer scales allowing to set up the model to the site conditions at these three levels. Two modelling case studies were designed. The first one was adapted to the site conditions withouth accounting for non-local effects and the second one considered the impact of a residual layer and advection into the system. The results for the latent heat flux were satisfactory at field scale as it was tuned towards a good representation of the surface layer scale, proving the importance of having information of transpiration and evaporation at leaf and surface scale. The modelled sensible heat flux depicts an overestimation of the measurements at a surface scale as it was tuned towards a good representation of the landscape scale. The boundary layer height, specific humidity and potential temperature in the mixed-layer were reproduced satisfactorily by CLASS after adding the effect of advection of warmer and drier air into the system and the effect of a residual layer. We conclude that the complete set of measurements at different scales is essential for the study of the vegetation-atmosphere interactions, although the heterogeneity of a landscape is still a challenge for the definition of processes at surface and correctly modelling all the scales.

Keywords: vegetation, mixed-layer, leaf, transpiration, surface fluxes

Contents

1. INTRODUCTION

1.1 BACKGROUND

Plants play an important role in the partition of available radiative energy into heat and water fluxes in the vegetation-atmosphere system. They respond to photosynthetically active radiation (PAR) to do photosynthesis by opening their stomata controlling the assimilation of CO_2. Plants respond to complex environmental conditions by adapting their stomata to temperature, atmospheric vapor deficit (VPD), internal and external CO_2 concentration and the leaf water potential [1, 2]. Stomata are the main path for the assimilation of CO_2 but also for water vapor that is released to the atmosphere. Every time that plants do photosynthesis they unavoidably lose water [3]. For this reason, stomatal behavior has an effect on the transport of water to the atmosphere, and as consequence on the formation of clouds, which depend on the turbulent transport of moisture and heat [4].

The surface is the main driver in the evolution of the diurnal boundary layer. Herein we rely on having a proper representation of the surface energy budget to have a best representation of the boundary layer [5]. It is not straightforward to make a connection between these two interconnected systems since there is not a direct, nor linear response on the complex processes that take place. One of the major problems is related to the horizontal and vertical scales involved in the exchange of water and heat (Figure 1.1). We need to move from the transpiration of a plant with a ~1m scale in the horizontal and vertical, to a field with a ~100m scale that feeds a surface layer that can extend to ~100m in the vertical and finally to a landscape with ~1-10km scale feeding a boundary layer that can grow to ~1km. Heterogeneity within the landscape scale adds complexity in the scaling considering the development of circulations due to differences in temperature transported from the surface. As consequence, the boundary layer properties change. Circulations are difficult to represent and parameterizations to understand these effects are still under study [6]. Due to this complexity, theories or models always require spatial averaging [7]. Is not surprising that studies in the last decade have focused on filling the gaps present in the integration of the land-atmosphere exchange processes both in observation and modelling [8]. In spite of major advances in understanding the land-atmosphere system [9-13] this is still a challenge.

With this study we aim to improve the understanding of the vegetation-atmosphere system by integrating in a 0-D model measurements at different scales from a multidisciplinary observation campaign.
From May to July of 2018, a campaign called CloudRoots was performed in Selhausen, Germany over a wheat crop (50.9° N, 6.4° E, 103 m.a.s.l.). Figure 1.2 is a satellite image of the 7th of May 2018, the selected day under study, showing the location of the wheat field at a landscape scale. We observe that there is a combination of green fields and bare soil or matured vegetation fields revealing clearly the heterogeneity present in the landscape and pose a major challenge representing the processes at boundary layer and landscape scales.

The purpose of the CloudRoots campaign was to improve and evaluate models in the land-atmosphere system by making an intensive collection of data at leaf, surface and boundary layer scales. It is this level of detailed information what makes this study unique, since we required such a comprehensive data-set to make the connection of measurements of moisture and heat from a leaf to a boundary layer scale. In the next chapter we present a complete description of the site and the data collected.

In order to integrate the measurements, we used CLASS. It is a 0-D land-atmospheric boundary layer model based on the mixed-layer equations to obtain the temporal evolution of the boundary layer and surface processes (Appendix A) [14]. The importance of using CLASS is that it has modules at the different scales of the vegetation-atmosphere system. For the transpiration at leaf scale it has the A-gs (assimilation-stomata conductance) module. For the surface scale, CLASS has a land-surface scheme. Furthermore, it is based on the mixed layer theory, therefore it reproduces a diurnal variability of variables as temperature, humidity, surface fluxes and boundary layer-dynamics.

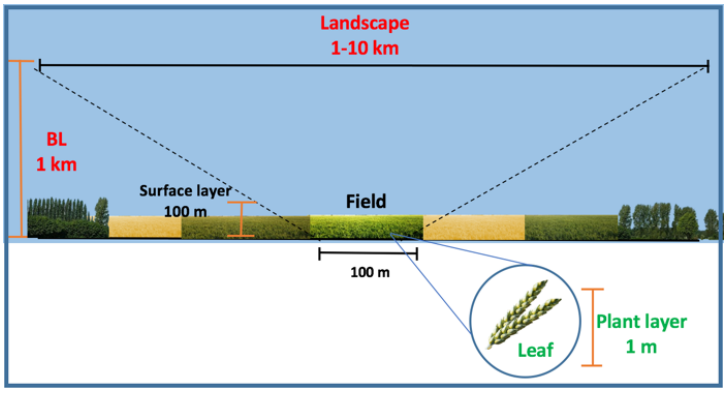

Figure 1.1 Vertical and horizontal scales involved in the vegetation-atmosphere system

Figure 1.2 Satellite image of the site on May 7th 2018

1.2 PROBLEM STATEMENT

The measurement and modelling of the interactions in the vegetation-atmosphere system is complex because there is not a linear connection between these two systems. This is related to the different spatial-temporal scales involved. Although in the last decades, multidisciplinary observational campaigns have been performed, there are still gaps in the integration of these processes. Therefore, we are interested in finding to what extent, observations at different scales improve the representation of the vegetation-atmosphere system using a 0-D model over a heterogeneous area.

1.3 RESEARCH QUESTIONS

The main research question is:

How do we integrate the field scales processes with the boundary layer dynamics?

To answer this question we sub-divide the research into three questions which include the key aspects we want to understand with our study:

1. To what extent do detailed field scale measurements improve the 0-D representation of the processes of plant to boundary layer scales?
2. Can we reproduce the boundary layer dynamics with a 0-D model over a heterogeneous terrain?
3. Can we reproduce the plant and field scale processes with a 0-D model at a single field within a heterogeneous terrain?

2. METHODOLODY

In this chapter we describe in Section 2.1 the data collected in the campaign. In Section 2.2 we give a description of the site. In Section 2.3 we present the case study strategy in CLASS and finally in Section 2.4 we describe the set-up of the case studies made in CLASS.

2.1 DATA DESCRIPTION

During the two months of the CloudRoots campaign (May to July of 2018) over a wheat crop in Selhausen, measurements at leaf, surface, and boundary layer scale were taken. Table 2.1 shows a summary of these measurements and the modules in CLASS with which they can be related.

Table 2.1 Data collected in the CloudRoots campaign

Scale	Measurements	CLASS module
Plant layer	• Gas exchange (Assimilation of CO_2 and transpiration) • Sap flow • Stomatal conductivity	**A-gs**
Surface layer	• Incoming and outgoing short-wave radiation, incoming and outgoing long-wave radiation. • Surface fluxes: Sensible heat (H), Latent heat (LE), soil (G) and CO_2 fluxes • Soil moisture at 6 depths from 0.01m to 1m • Profiles of wind speed, temperature, H_2O and CO_2 up to 2m • Isotopes of H_2O and CO_2 • Biomass using Cosmic Ray Neutron Sensing • Precipitation	**Land surface scheme**
Boundary layer	• Remote sensing (Radiosonde data) of temperature and specific humidity from Essen, Germany. • Doppler wind LIDAR data of wind speed and boundary layer height (Jülich) • Microwave data of boundary layer height and temperature (JOYCE) • Solar-induced fluorescence from ground, aircraft and satellite level	**Mixed-layer**

2.1.1 Leaf layer

The gas exchange at leaf scale was measured with a LiCor LI-6400XT (Figure 2.1) during the 3 IOPs (Intensive Observation Period) of the campaign: 7th of May, 15th and 28th of June. Two IRGAs (InfraRed Gas Analyzer) measures the change in CO_2 and water vapor concentration in

the airflow across the leaf, giving information on stomatal conductance, photosynthesis and transpiration. This allows to have light and CO_2 responses of photosynthesis that were used for the set-up of the land surface model in CLASS. The purpose was to adapt the model to the site conditions in order to have transpiration representative of the site.

We also had information of sap flow from a micro-sensor designed by Dynamax Inc. that measures differences in temperature in a stem section that is thermally insulated and constantly heated [15]. The measurements also provide information of transpiration at leaf scale. LAI was also determined for the site. This is important for the upscaling to a canopy/surface layer in the model.

Figure 2.1 LI-6400XT used in the CloudRoots campaign to measure the leaf gas exchange

2.1.2 Surface layer

Measurements of surface temperature, wind speed (three components *u*, *v* and *w*), water vapor and CO_2 concentrations were collected with an Eddy-Covariance system placed in the field at 2m above soil level (Figure 2.2). The surface fluxes H and LE were calculated and processed using EddyPro and determined in a 30min time scale. Water vapor and CO_2 were determined with an open-path IRGA LI7500. A three dimensional (x, y, z) sonic anemometer CSAT3 measures the wind speed. H and LE determined with the Eddy-Covariance were compared with the ones simulated by CLASS. Furthermore, the measurements of temperature and specific humidity were used as reference for set up the initial conditions in the model. Net radiation was also measured with radiometers (Kipp and Zonen CM14 and CG2).

We also had data of water vapor and CO_2 concentration, surface temperature and wind speed from an Eddy-Covariance located at ~500m from our site over a bare-soil field. This is important to observe the differences in the surface fluxes between our field and another close to our site that has a contrasting land surface.

An elevator-based facility [16] was installed on the site. It moves from surface to a level of 2m taking measurements of temperature, wind speed, CO_2 and water vapor with a resolution of 2.5cm and 20Hz . This is useful for the definition of the profiles of these variables.

In addition, we had measurements of soil temperature and soil water content. They were determined from sensors distributed at four points over the field to better quantify the heterogeneity of this variable. The intention was to characterize soil properties in deeper layers, thus, they were buried at 6 depths (1cm, 5cm, 10cm, 20cm, 50cm and 1m). Two heat flux plates were buried at ~5cm depth to determine the ground flux. Furthermore, we had the description of the soil type (content of clay, sand, silt and organic carbon content), as well as soil respiration with an automated Li8100 system. More over there was a quantification of biomass by using cosmic-ray neutron sensing to understand the dynamics and feedback between the soil water content and biomass production [17].

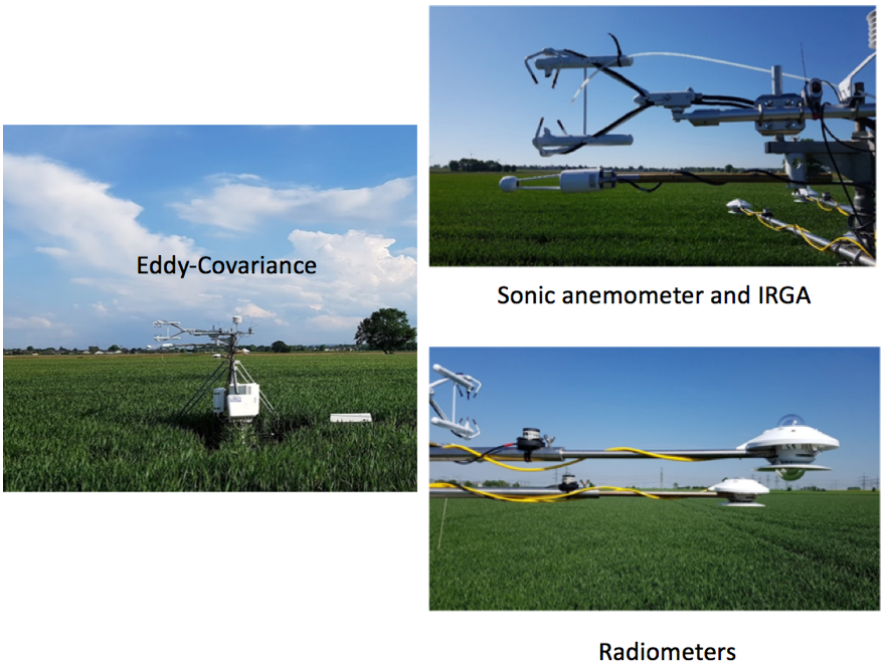

Figure 2.2 Equipment at Selhausen site for surface layer measurements

Isotopologues and isofluxes of water vapor and carbon were measured with a mobile isotope analyzer system to quantify the contributions at leaf, surface and boundary layers and for the determination of the mixing ratio and diurnal variability.

2.1.3 Boundary layer

Along with the collection of surface data in the campaign, we had available information at a boundary layer scale from radiosonde (RS) launches in Essen (~70km from site) and from the Jülich Observatory for Cloud Evolution (JOYCE) (~10km from site). The radiosonde provided data at 00:00 UTC and at 12:00 UTC from 147m to 30 km height. It covers information of temperature, wind speed, pressure, relative humidity and mixing ratio.

The JOYCE facility monitors wind, temperature, water vapor, clouds and precipitation since 2011. The instruments in the JOYCE facility are:

- Atmospheric Emitted Radiance Interferometer (AERI)
- Ceilometer CT25K
- Cloud Radar JOYRAD-35 JOYRAD-94
- Microwave Radiometer HATPRO-TOPHAT
- Doppler Wind LIDAR
- Micro Rain Radar
- Multifilter Rotating Shadowband Radiometer
- Sodar
- Total Sky Imager

We used data from the Microwave Radiometer (MR) that contains temperature and humidity profiles from surface to 10km height with a resolution of 50m and 1 second time step, as well as integrated water vapor and liquid water path. We also used measurements of wind speed and boundary layer height with the Doppler wind LIDAR (Laser Imaging Detection and Ranging) from surface to 9km height with a resolution of 30m and 15min time step.

A large scale mapping of the field heterogeneity was made showing various vegetation types based on measurements of solar-induced fluorescence with an airborne imaging spectrometer Hyplant [18]. This is an indicator for photosynthetic efficiency and it can be related to variation of photosynthesis.

2.2 SITE DESCRIPTION

The Selhausen site represents the heterogeneous agricultural rural area of the lower Rhine valley in Germany. The annual averaged temperature and precipitation are 11°C and 655mm respectively. The most important crops in the region are sugar beet, winter wheat, winter barley, maize and rape seed. Only parts of the region are managed as grasslands. The CloudRoots campaign was performed in this region over a winter wheat field (Figure 1.2). We selected the 7th of May 2018 for our study because it is a golden day with no influence of clouds.

The heterogeneity of the landscape adds complexity to our study. Figure 1.2 shows the mosaic that surrounds our field, suggesting that different surface fluxes are contributing to the characterization of the boundary layer. In order to illustrate the variability Figure 2.3 shows the surface fluxes of a) the bare-soil field close to our site (~500m), b) the wheat crop field of study, and c) an estimate made based on a classification of areas in the landscape. The estimate considered that the landscape is divided into 40% green areas and 60% bare soil or matured vegetation areas using as reference the satellite image of the day under study (Figure 1.2b). We also estimated that the surface fluxes of the green areas are similar to the ones to our field, while for the rest are similar to the nearby site. The fluxes correspond to the 25th of May 2018 and were measured with an Eddy-Covariance. We observe that the fluxes at both sites are considerably different. The Bowen ratio for the nearby site with characteristics of a bare soil is 0.83 on average whereas for the wheat crop it is 0.28, where most of the energy is used for

evapotranspiration. The bowen ratio for the landscape would be of 0.43. This represents one of the challenges for the connection of surface processes with the boundary layer dynamics.

Figure 2.4 is a weather map of the day of our study, the 7th of May. We observe that there is a high pressure system located at the north of Poland. This suggests that advection at a synoptic scale can be developed. The wind from south-east, brings warm and dry air. Therefore, the location of the high pressure system can enhance the advection of air with these conditions to our site, having an impact on the boundary layer properties. Although, the presence of the high pressure system also suggests an advection at a boundary layer scale since the wind imposed on our fields by large scale forcing moves warmer and drier air from the bare-soil/matured vegetation fields to our wheat field, and likewise this wind moves cooler and moister air from our field to the next ones.

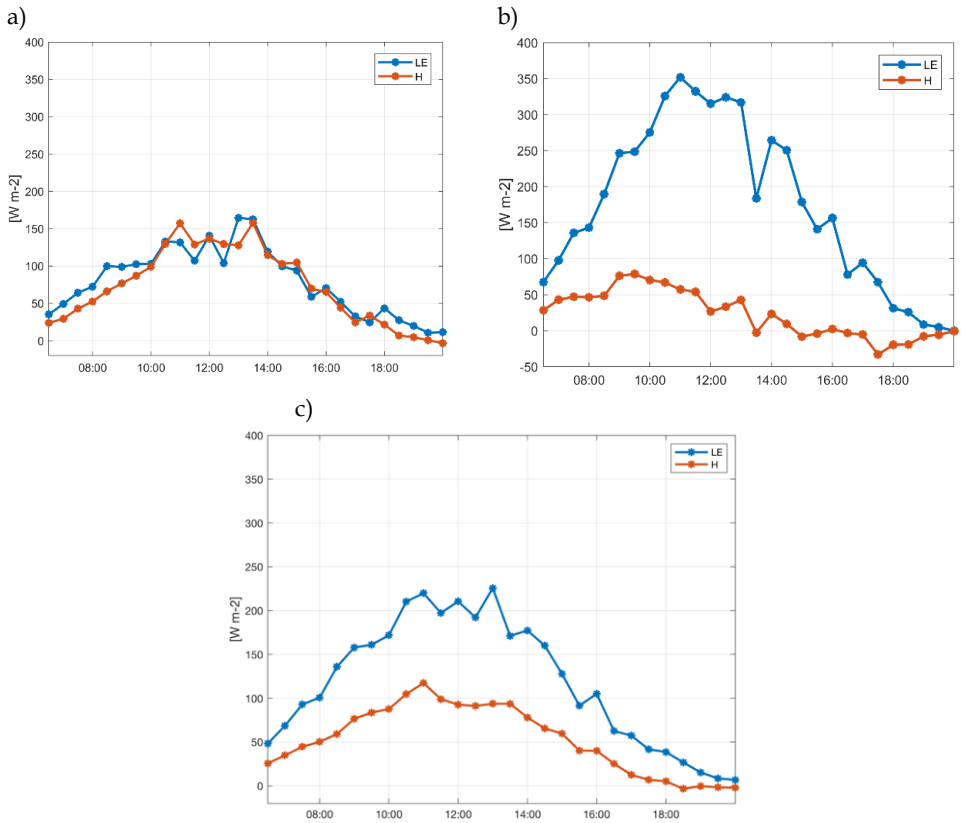

Figure 2.3. a) Surface fluxes of a nearby site b) surface fluxes of the field of study and c) estimated landscape fluxes

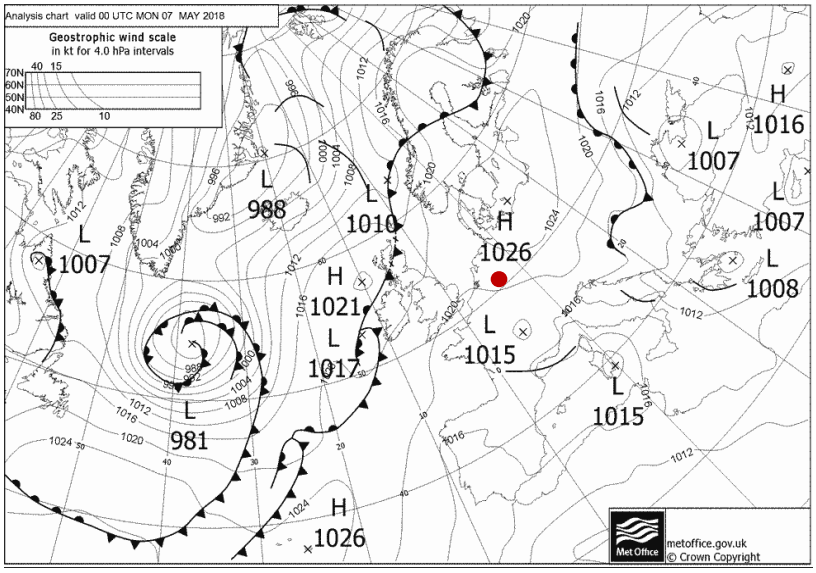

Figure 2.4 Weather map for the 7th of May 2018. The location of Selhausen is marked with the red dot

2.3 CASE STUDIES

We were interested in knowing to what extent a 0-D model reproduces processes at surface and connect them with the boundary layer dynamics based on detailed measurements at different scales. In order to achieve this in this study, we had to consider four important aspects:

1. **Heterogeneity of the landscape**. The objective was to represent the surface fluxes and connect them with the boundary layer dynamics. We need to consider a landscape scale in which not only the turbulent transport of water vapor and heat from the wheat field, but from other fields change the properties of the boundary layer. We face the problem of moving between measurements at field scale to a landscape that is very heterogeneous (Section 2.2).
2. **Soil moisture and soil water retention characteristics**. Based on the observations we were able to define the water content at two different depths but more important, with the information of the soil type we could define the water content wilting point and field capacity of the soil which are essential for evapotranspiration since those are indicators of water available for the plant and the soil moisture specific for the site. These inputs for the model represent the field scale.
3. **Advection**. We also had to consider the impact of advection as presented in the previous section. The advection of drier and warmer air could originate on a synoptic scale or a boundary layer scale.
4. **Residual layer in the early morning**. As CLASS is a mixed-layer model it is not able to reproduce the processes that occur at night. However, the impact of the night conditions on the evolution of the diurnal boundary layer can be taken into account in prescribing the initial conditions. It was found that considering a residual layer in a large eddy simulation can reproduce the observed sudden increase in boundary layer depth during

the morning transition [19]. Additionally, it has been reported that when a neutral residual layer caps the convective boundary layer the growth of the latter is less determined by the surface fluxes and more by the lapse rate of the former [20].

2.3.1 Case Study Strategy

CLASS models the physics at surface considering a homogeneous area. Therefore, we knew beforehand that reproducing the surface fluxes for our site would be challenging as presented in Figure 1.3. Hence, in order to comply with the first aspect of the previous section, we decided to give priority to the representation of properties at the boundary layer scale. Moreover, for the other three aspects, we designed two case studies in CLASS:

1. Control (CTRL). In this case we adapted the model to the site observations at leaf, surface and boundary layer scales.
2. Adding a residual layer and advection (RL-ADV). This was defined as the Control but additionally we considered the impact on the system of two effects:

    - The residual layer (RL) in the early morning.
    - External forcing (advection of dry and warm air)

In the next section we present in detail how we set-up the two case studies in CLASS.

2.3.2 Control Case

The model was set-up to simulate 14 hours from 06:00 UTC until 20:00 UTC (08:00 until 22:00 CEST) with a time step of 1 second. As mentioned previously, we selected the 7th of May for the case study. We will describe the set up for each module in CLASS: **A-gs, land surface and mixed-layer**.

A-gs

Based on the leaf scale measurements of photosynthesis, response curves of assimilation with internal carbon concentration (A-ci) and of assimilation with PAR (A-PAR) were derived. In this module, the model was adapted to generate leaf gas exchange that is representative of the winter wheat. The model was adapted by changing three parameters: the light use efficiency, the mesophyll conductance at 298 K and the maximum photosynthesis at 298 K (Table 2.2).

Land surface

In this module, we defined the roughness length, albedo, leaf area index (LAI) and soil water content. We used data from observations giving priority to the representation of the LE . The roughness length for momentum was defined by typical rule of thumb as 10% of the canopy height of that day (.45m) minus a displacement (60% of the canopy height). The roughness

length for heat was considered to be 10% of the roughness length for momentum. The albedo was calculated from the radiation measurements and LAI was defined also based on measurements.

The soil water content was set according to measurements at .05m and at 0.1m. But by changing the water content according to the site, we needed to redefine the water content at field capacity (w_{fc}) and at wilting point (w_{wilt}). We determined these values calculating the water retention curve of the soil based on its type (% content of clay, silt and sand) [21]. CLASS uses this definition of soil moisture index (SMI) in its calculations for evapotranspiration:

$$\mathrm{SMI} = \frac{w_{surface} - w_{wilt}}{w_{fc} - w_{wilt}} \quad (1)$$

Initial mixed-layer

For the definition of conditions in the mixed-layer we assume that the boundary layer is representative of a large area (Figure 1.2b), therefore inspired by the radiosonde measurements at 00:00 UTC (Figure 2.5) we defined the initial conditions of potential temperature and specific humidity. Even though CLASS starts the simulation at 06:00 UTC, the conditions at 00:00 UTC were used as approximate initial values for the mixed-layer. Table 2.2 contains an overview of the variables and values set-up in CLASS.

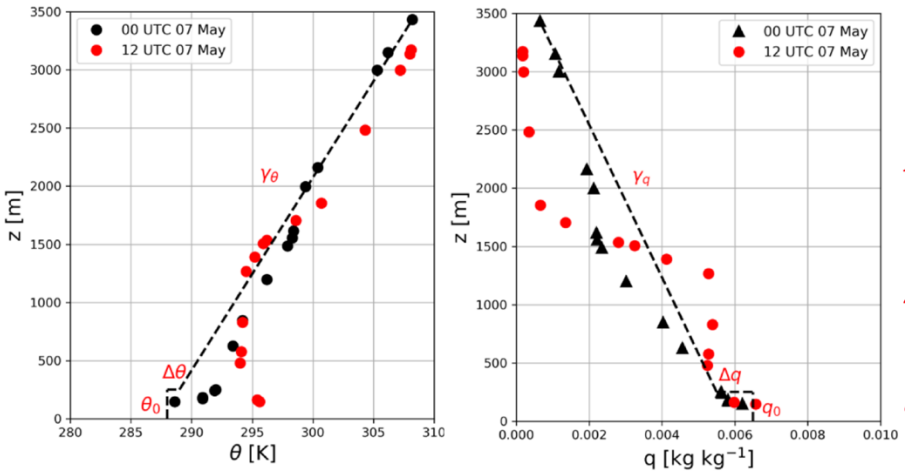

Figure 2.5 RS measurements available at 00:00 UTC and 12 :00 UTC for the 7th May 2018

From measurements of the Doppler wind LIDAR and the Microwave Radiometer, we determined the well mixed wind speed and the initial boundary layer height.

Table 2.2 Overview of set up of variables in CLASS for the Control case

Variable	**Value**
Light use efficiency [mg J^{-1}]	0.0053
Mesophyll conductance at 298K [mm s]	10
Max. photosynthesis at 298K [mg $m^{-2}s^{-1}$]	1.926

Initial ABL height [m]	135
Initial θ [K]	286
Initial Δθ [K]	2
Lapse rate θ [Km^{-1}]	0.006
Advection of heat [$K\ h^{-1}$]	0
Initial q [$g\ kg^{-1}$]	5.3
Initial Δq [$g\ kg^{-1}$]	-0.02
Lapse rate q [$g\ kg^{-1}m^{-1}$]	0
Advection of moisture [$g\ kg\ h^{-1}$]	0
Initial wind speed (u) [ms^{-1}]	-5
Initial wind speed (v) [ms^{-1}]	5
Ustar [ms^{-1}]	0.3
Roughness length (z0m) [m]	.012
Roughness length (z0h) [m]	0.0012
Water content top layer [m^3m^{-3}]	0.178
Water content deeper layer [m^3m^{-3}]	0.286
Temperature top soil layer [K]	285
Temperature deeper soil layer [K]	286
Water content field capacity [-]	0.3
Water content wilting point [-]	0.154
LAI [-]	5
Albedo [-]	0.2

2.3.3 Residual layer and Advection (RL-ADV) Case

CLASS is a mixed-layer model and therefore it is not able to reproduce the processes that occur at night. Due to this we are starting our day in CLASS missing the characteristics of the previous day decayed mixed-layer contained in a residual layer (RL). To overcome and solve the role of a residual layer, we defined different lapse rate for temperature after 12:00 UTC inspired in the remote sensing measurements considering that before this time we had values that correspond to the RL. Due to the small change in the lapse rate for specific humidity we kept its same initial value.

We added the advection of heat and dry air into our system based on the following equation budgets:

$$\frac{\Delta<\theta>}{\Delta t} = \frac{1}{\rho C_p}\frac{\Delta H}{h} + u\frac{\Delta<\theta>}{\Delta x} \quad (2)$$

$$\frac{\Delta<q>}{\Delta t} = \frac{1}{\rho L_v}\frac{\Delta LE}{h} + u\frac{\Delta<q>}{\Delta x} \quad (3)$$

Equation (2) represents the temporal evolution of the temperature budget in our system impacted by two terms: 1) the change in the surface kinematic heat flux with height that gives

us an estimate of the boundary layer heat rate (first term on the right hand side of the equation) and 2) the large scale wind moving warmer air from other fields to ours and moving cooler air from our field to the next ones. Similarly, Equation (3) represents the temporal evolution of the specific humidity budget in our system impacted by the change in the surface kinematic moisture flux with height that gives us an estimate of the boundary layer moisture rate and the large scale wind moving drier air from other fields to ours and moister air from our field to the next ones. We defined the terms of the previous equations to prescribe the advection which is at a boundary layer scale (Figure 2.6) inspired by the measurements of potential temperature, specific humidity and surface fluxes at the wheat and bare-soil fields.

We took as reference the Microwave measurements to define the temporal evolution of the potential temperature. The boundary layer scale advection of heat we prescribed has a maximum at 11:30 UTC. At this time, the temperature changes 0.24 [$\mathrm{K\,h^{-1}}$]. We used the sensible heat flux we estimated for the landscape (Figure 2.3c) and the measurements of boundary layer height as reference for the first term on the right hand of the equation. At 11:30 UTC this term is (-0.22 [$\mathrm{K\,h^{-1}}$]) considering a boundary layer height of 1335m and that the surface fluxes are zero at the boundary layer height. Therefore, we get advection of 0.467 [$\mathrm{K\,h^{-1}}$] by 11:30 UTC.

Similarly, for the specific humidity we had the temporal evolution from the Eddy-covariance measurements and estimated a 20% less than measured at surface considering that this quantity is higher at surface to got values at the boundary layer height. The specific humidity changed -0.465[$\mathrm{g\ kg^{-1}\ h^{-1}}$] by 11:30 UTC. We used the latent heat flux we estimated for the landscape (Figure 2.3c) to obtain the first term on the right hand of the equation (-0.194[$\mathrm{g\ kg^{-1}\ h^{-1}}$]). Therefore, we get advection of -0.27 [$\mathrm{g\ kg^{-1}\ h^{-1}}$] by 11:30 UTC.

We prescribed higher advection values for temperature and specific humidity but in the same order of magnitude as the values we obtained from the equation. For the advection of heat we prescribed a maximum of 0.72 [$\mathrm{K\,h^{-1}}$] by 11:30 UTC compared to 0.467 [$\mathrm{K\,h^{-1}}$]. For the advection of moisture, we prescribed -0.65 [g kg-1 h-1] at 11:30 UTC compared to -0.27 [$\mathrm{g\ kg^{-1}\ h^{-1}}$]. This is because we were considering only the comparison between our field and the bare soil field. Hence, as we mentioned previously, we gave priority to the representation of the boundary layer scale (Section 2.3) and we need to consider the contribution to the evolution of the boundary layer properties from other fields present in the landscape in which we estimated that 60% of the areas have characteristics of a bare soil or matured vegetated fields (Section 2.2). Furthermore, we prescribed a gradual advection, inspired on the differences we found in the kinematic fluxes between the wheat field and the bare soil for the 25th of May 2018 (Figure 2.7). This was a reference for the evolution of the advection of warmer and drier air in our system considering the heterogeneity of the landscape.

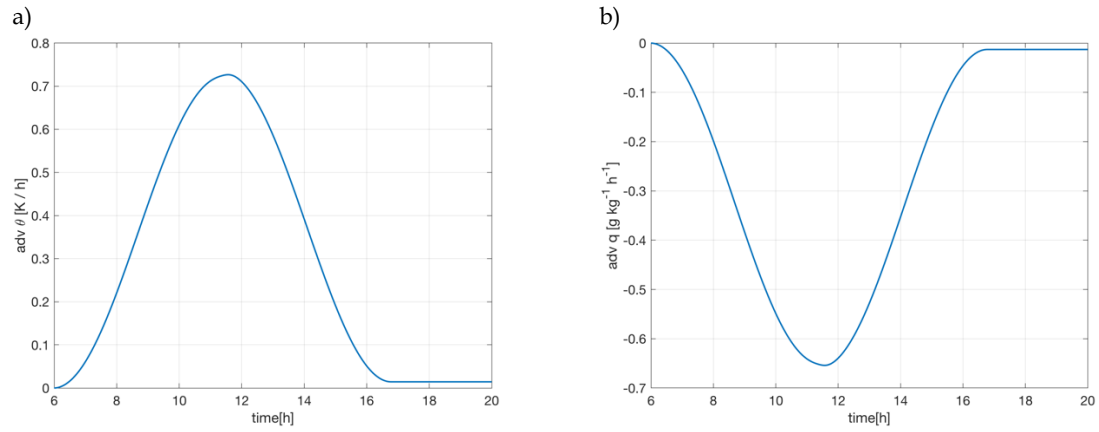

Figure 2.6 a) Advection of heat and b) dry air

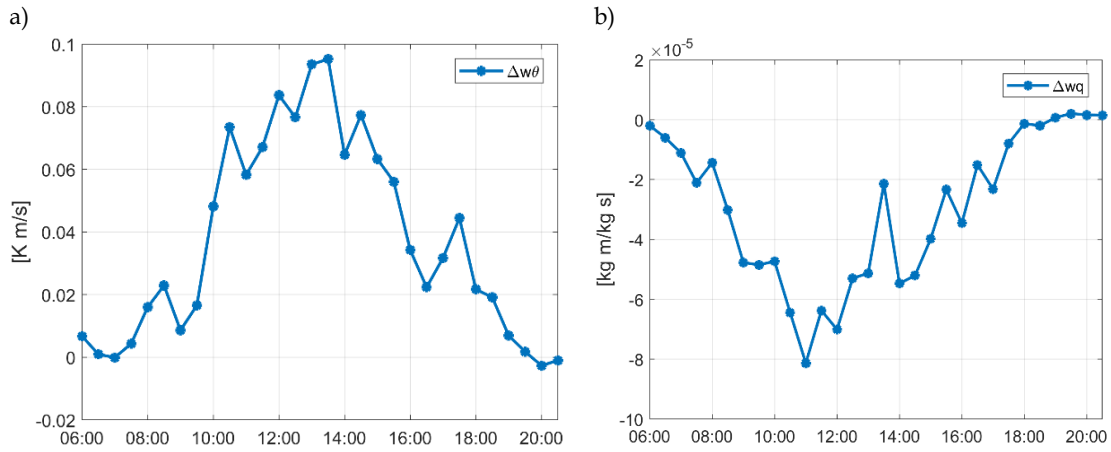

Figure 2.7 Difference in a) the surface kinematic heat flux ($\overline{w'\theta'}$) and b) the surface kinematic moisture flux ($\overline{w'q'}$) between the bare soil and our wheat crop

3. RESULTS

3.1 CONTROL CASE

In this case study, CLASS was adapted to the site conditions of the CloudRoots campaign. To have a better understanding of how the model is representing the field processes and the boundary layer dynamics, we first show the results of the available net radiation and the variables at surface since the boundary layer dynamics depend strongly on the surface conditions.

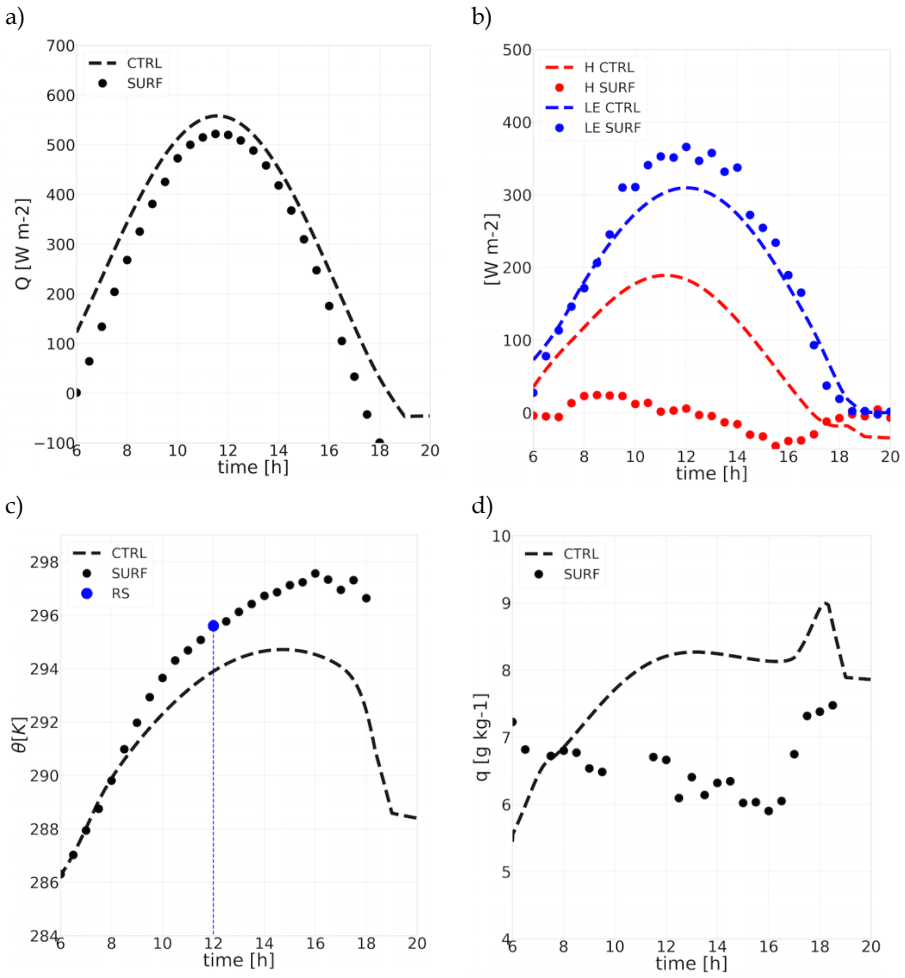

Figure 3.1 Net Radiation (a), Surface Fluxes (b), Temperature at 2m (c) and specific humidity at 2m (d) for control run (CTRL) compared to measurements at 2m (SURF) and radiosonde (RS)

We observe that the net Radiation is slightly overestimated but comparable to observations (Figure 3.1a). We also see that at surface scale we have a good representation of the latent heat flux (LE) despite an underestimation around midday that can be improved. This result proves the benefit of using input with such detailed information at plant and surface scale in the representation of evapotranspiration at surface scale. From leaf gas exchange measurements, we defined parameters in the model in order to have the transpiration reliable to be

representative for the site. Furtheremore, we consider our field to be mostly covered by vegetation and this is the reason why the up-scaling of transpiration made in CLASS to a canopy using the "big leaf" scheme is represented acquaretly. Moreover, we provided to the model a definition of soil moisture and the soil water content wilting point and field capacity that we also adapted based on measurements and soil type of the site. Due to the availability of data the results for evapotranspiration were comparable to the observations at surface scale. On the other hand, there is a significant overestimation of sensible heat flux (H). The reason for this difference is that we are comparing values of H that the model tries to mimic at a landscape scale against observations at field scale that are representative only of our wheat crop field. We don't have landscape scale flux measurements, although due to the heterogeneity of the landscape this result is tuned towards a good representation at the landscape scale. A future research can consider the effect of forcing a higher H in CLASS, but this is still a challenge if we don't have references from more fields.

The temperature at 2m increases fast in the morning and it is comparable to observations although, it shows an underestimation from 09:00 UTC (Figure 3.1c). This will be discussed further in the case study with advection. Even though it is important to notice that the radiosonde shows the same temperature at midday as the surface measurements despite its location (~70km from site). Last, we observe that the model makes an overestimation of specific humidity (Figure 3.1d). It could be caused by low entrainment rate related to a high specific humidity jump at the boundary layer height. It is interesting to notice that there is a peak in the representation of the specific humidity around 17:00 UTC and that it is also seen in the measurements. It can be explained by H becoming negative by that time and LE being still positive. This means that in CLASS we are still adding moisture to the boundary layer even though the site conditions were becoming stable.

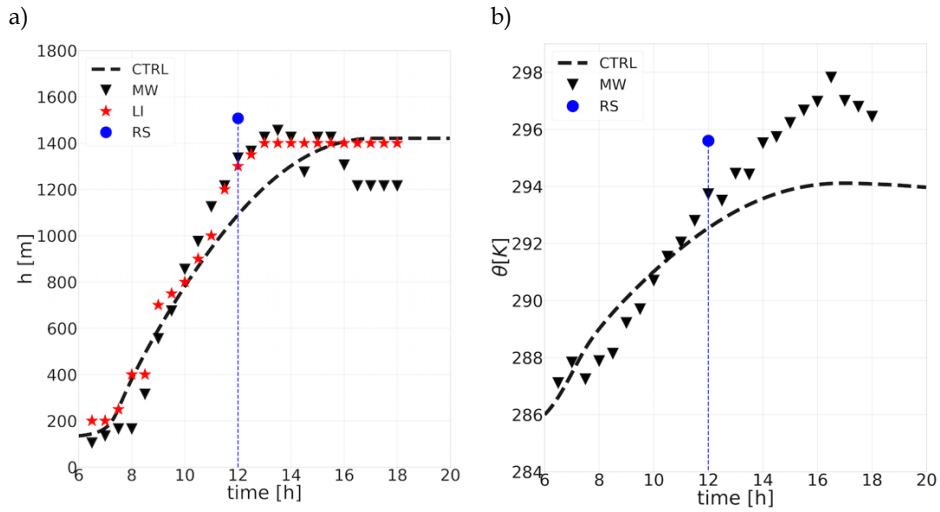

Figure 3.2 Boundary layer height (a) and potential temperature in the boundary layer (b) for control run (CTRL) compared to Microwave (MW), LIDAR (LI) and radiosonde (RS) measurements.

In Figure 3.2 we observe the results at the boundary layer scale. We see that the boundary layer height is close to the observations in the early morning but it also makes an underestimation before 16:00 UTC and after this time its growth ceases (Figure 3.2a) because the surface fluxes are decreasing in the afternoon limiting the source of heat. This could also be an explanation for the peak we observe for the specific humidity at surface (Figure 3.1d) because the system keeps adding moisture to the system in a boundary layer that stopped increasing leading to a sudden increase of specific humidity. The radiosonde shows a boundary layer depth of 1500 m at 12:00 UTC, that is comparable to the microwave and LIDAR observations at the same time. The potential temperature is underestimated compared to measurements and it also stops increasing after 16:00 UTC (Figure 3.2b). We observe a fast increase in potential temperature in the early morning due to the shallow boundary layer at this time. As the boundary layer grows, the potential temperature increases less. The effect of this growth evolution of the boundary layer is also seen Figure 3.1b and Figure 3.1c.

The results of the case study show that there is not enough heat in the system to reach the measurements of the boundary layer properties, surface temperature and specific humidity. Although, LE is comparable to the observations and it can still be improved.

3.2 RESIDUAL LAYER AND ADVECTION CASE

For this case study, we will first show the effect of re-defining the lapse rate and adding advection of heat. Later, we will show the impact of adding advection of dry air.

When a residual layer is present with a shallow boundary layer in the early morning, the connection between these two occurs with a process called overshooting in which the buoyant thermals at surface rise directly to the residual layer resulting in a very fast mixing of the new boundary layer with the air masses in the residual layer. After this moment the potential temperature in both layers is equal and the mixed layer theory can be applied [22].

In order to implement the presence of the two layers in our case we defined a lapse rate for each layer. Previously, the lapse rate of potential temperature had a constant value of 0.006 [K m-1] (Table 2.2). In this run we defined a gradual change at 12:00 UTC until it reaches a value of of .008 [K m-1]. When we increase the lapse rate, it limits the boundary layer growth. At the same time, it has an effect on the potential temperature jump at inversion, reducing the entrainment. Furthermore, we added a gradual advection of heat with a maximum of 0.72 [K h-1] at 11:30 UTC. The definition of these variables are shown Figure 3.3.
We observe in Figure 3.4 that by adding advection of warmer air at a boundary layer scale, we decrease the transfer of heat from the surface compared to the Control run and because the surface still is warming during the day, the temperature increases. The representation of temperature at 2m is improved. We observe that it reaches the same value as the radiosonde at 12:00 UTC and it increases less after this time. On the other hand, the specific humidity doesn't change considerably, although after the change in the lapse rate of temperature, the specific humidity increases and this is realted to the lower entrainment of dry air to the system.

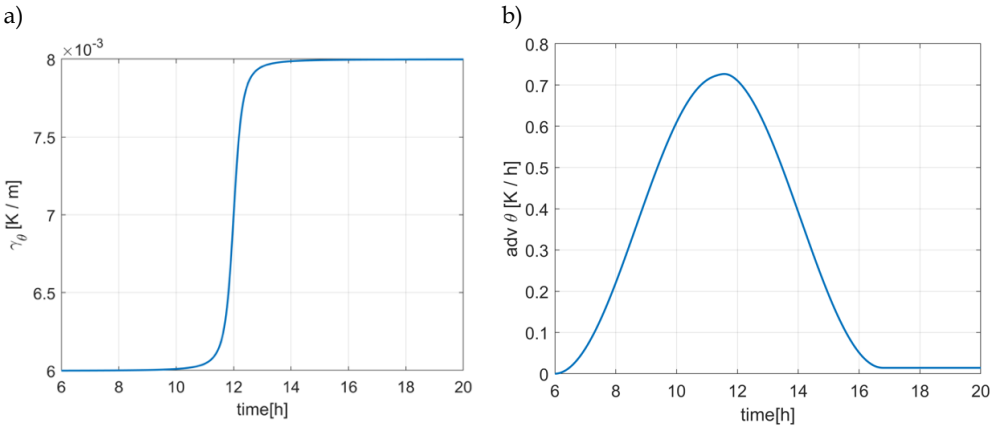

Figure 3.3 Potential temperature lapse rate (a) and advection of heat (b) defined for the RL-ADV run

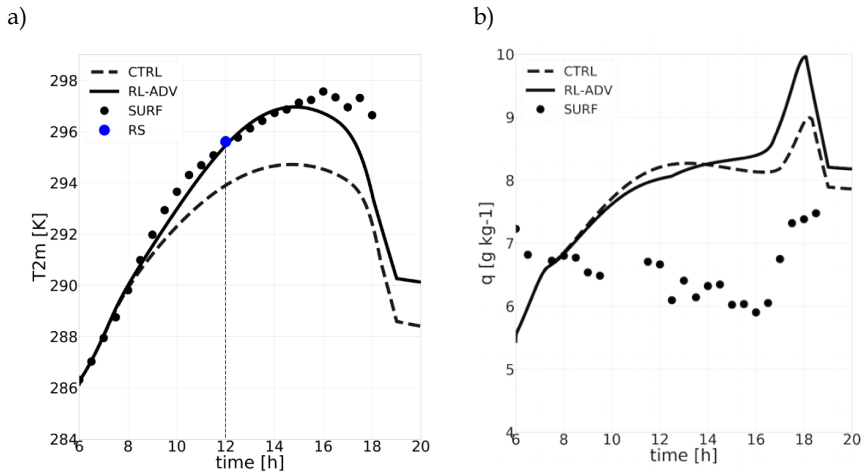

Figure 3.4 Temperature at 2m (a) and specific humidity at 2m (b) for RL-ADV run compared to control run (CTRL) and measurements

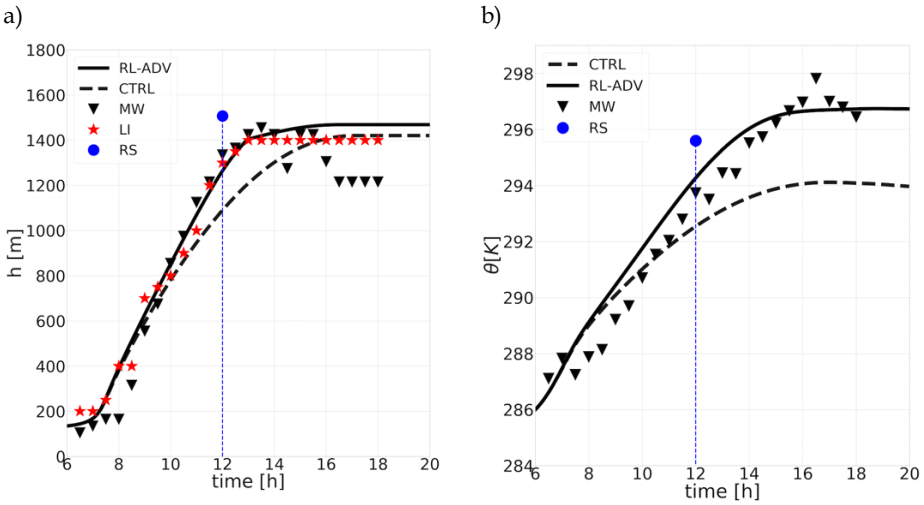

Figure 3.5 Boundary layer height (a) and potential temperature (b) for RL-ADV run compared to control run (CTRL) and measurements

We observe in Figure 3.5 that with this magnitude of advection of heat we prescribed, we allow the higher growth of the boundary layer depth and the potential temperature. Before 12:00 UTC the entrainment is still active and together with the addition of heat by boundary layer scale advection (Equation 2 in Section 2.3.3), we increase the potential temperature and boundary layer depth. Defining a higher lapse rate after 12:00 UTC makes that the BL stops growing despite the advection of heat. If the boundary layer stops increasing we can expect that the potential temperature would increase, but because we defined a gradual advection of heat, its growth ceases as well. When we reduce the entrainment by increasing the lapse rate we also reduce H.

Furthermore, we added advection of dry air as shown in Figure 3.6a. The advection prescribed has a maximum of -0.65 [g kg-1 h-1] at 11:30 UTC.

As it was expected, after adding advection of drier air in the system, we noticed that the specific humidity changes considerably as shown in Figure 3.6b. The advection has an effect on LE, because we are decreasing the mixed-layer specific humidity. This means that we increase the transport of water vapor from surface to the atmosphere and this is reflected in the decrease of the specific humidity at surface. Therefore, the plot shows the connection between processes at the boundary layer scale (the advection of dry air) with the processes that occur at surface scale (the change in the vertical transport of specific humidity from the surface to the atmosphere).The representation is comparable to the observations. It is important to notice that the peak around 18:00 UTC is still reproduced by the model.

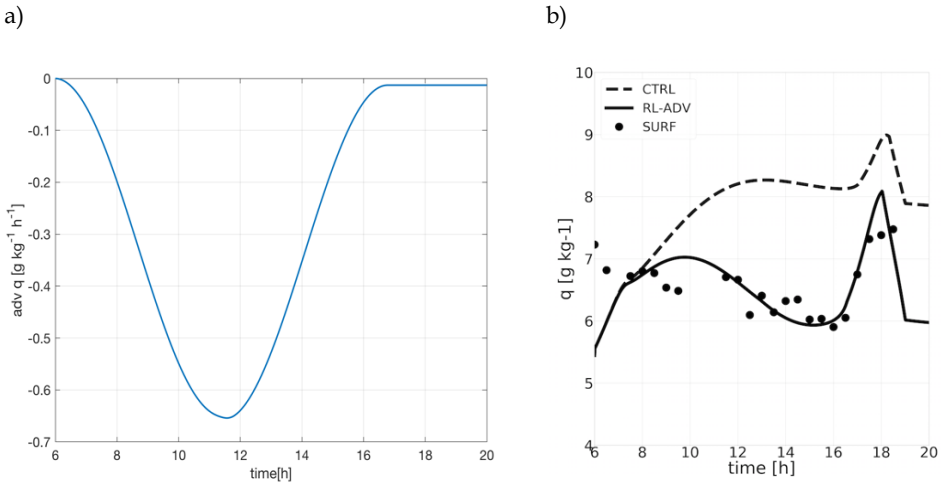

Figure 3.6 Advection of dry air (a) and specific humidity at 2m for RL-ADV run compared to control run and measurements

The representation of boundary layer height, specific humidity at surface and temperature at surface and boundary layer scales after adding advection prescribed based on the differences in the kinematic flux of temperature and specific humidity between the bare-soil field and our field proves that we had a case of addvection at a boundary layer scale.

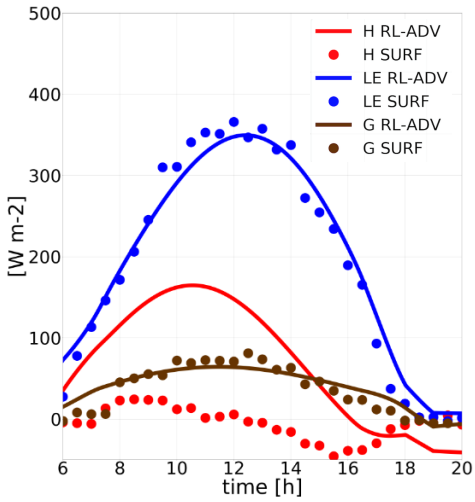

Figure 3.7 Surface fluxes for the RL-ADV run compared to control run

Figure 3.7 depicts the final results for the surface fluxes. By adding advection of heat at the boundary layer scale to the system, we are prescribing the effect of the heterogeneity in the landscape (Section 2.2), that compared to the control case has an impact on the surface and boundary layer scales. LE increased as consequence of the presence of drier air in the boundary layer, having a final satisfactory result. H is 15% lower compared to the Control case study and we see that is more comparable to the estimation of H we did in Section 2.2 (Figure 2.3 c). The ground flux shows as well comparable values to the observations.

4. DISCUSSION

With this study we learned the importance of having detailed measurements at different scales. Having a collection of data from the multidisciplinary campaign CloudRoots improves the understanding and the representation of the coupling between the vegetation and the atmosphere. Because we had detailed information at a plant and surface scale it was challenging to connect the processes at this scales with the exchange of water and heat at a landscape and boundary layer scales. Despite this, we implemented a novel work in the 0-D model CLASS to integrate the measurements. Even though we had information at a boundary layer scale to set up the model, the results from the Control run showed that we required to add information at a boundary layer scale in the 0-D model CLASS to represent the effects of having a heterogeneous landscape and a residual layer. Therefore we were forced to implement additional forcings in order to input to the model the conditions at landscape and boundary layer scale.

This study shows that the vegetation and atmoshpere responses are dependent on spatio-temporal scales and therefore is not straightforward to integrate this system and even more difficult to try to analyze it over a heterogeneous landscape. Even though, the results after adding a residual layer and the advection of warmer and drier air show to be comparable to observations and lead to a good representation of variables at plant, surface and boundary layer scales. In our case studies we observed that changes at the boundary layer scale as the advection or the entrainment has effects in the potential temperature, specific humidity and heat fluxes at surface. This shows the constant feedback between the surface and the boundary layer dynamics and it is not only a connection from the surface as a source of water vapor and heat, but also in the other way around. This study could be improved if during the campaign we had more IOPs with measurements on clear days and also available information at other fields on the same days in order to have more references and a higher collection of data over the landscape.

The data collected from this campaign is rich enough to expand the study of the vegetation-atmosphere coupling. Future studies can focus on the development of clouds and the connection with processes at surface and plant scales. We learned that the way in which plants react to environmental conditions is very important for the definition of processes at surface, therefore, having a cloudy day instead of a clear day will give more information about how the surface fluxes change due to response of plants to clouds and even more, the feedback from plants to the formation of clouds. This can also be implemented and studied in CLASS since it has a module for clouds.

5. CONCLUSIONS

In this study we wanted to know to what extent, observations at different scales improve the representation of the vegetation-atmosphere system over a heterogeneous area. We did this by integrating the measurements at leaf, surface and boundary layer scale from an intensive campaign called CloudRoots performed over a wheat crop field in Selhausen, Germany from May to July of 2018. We integrated the observations and represented the surface processes and boundary layer dynamics by designing two modelling cases in the 0-D model CLASS. In the first case we adapted CLASS to the site condtions and in the second we considered the impact of a residual layer and advection to the system. We selected the 7th of May for our cases since it was a golden day with fair weather conditions and an intensive observation period.

CLASS considers an homogeneous surface and this represented a challenge. Even though, as a result of our first case study, we achieved satisfactory results of evapotranspiration at surface layer scale as a result of having such a detailed information of transpiration and evaporation at plant and surface scale. We found that it is this level of detailed information that improves the representation of surface processes. On the other hand, the results for the sensible heat flux show an overestimation compared to the observations at surface scale but the sensible heat flux was tuned towards a good representation of the landscape scale since we added advection of warmer and drier air as an external forcing into our system. This case study proves that providing detailed information of mixed-layer conditions to CLASS is important for defining the temporal evolution of properties at the boundary layer scale, although the results also showed that the system didn't have enough heat to reach the observations at the this scale.

In contrast, our second case study proved that CLASS is able to reproduce the boundary layer dynamics by changing the conditions in the early morning and by adding advection to the system. Furthermore, temperature and specific humidity at surface level were also improved. The results show that defining conditions of a residual layer in the early morning is important for satisfactory results. Complementary to this, as an effect of the landscape heterogeneity, we demonstrated that the site was under the influence of advection of warm and dry air at a boundary layer scale. This is because the advection we prescribed in our case inspired on the differences in the kinematic heat flux and kinematic moisture flux between our field and a bare-soil field close to our site improved the representation of the potential temperature, specific humidity and the boundary layer growth.
The results of this study indicate that the integration of measurements at leaf, surface and boundary layer scale was essential for the good representation of processes connecting these three levels. Using the 0-D model CLASS helped us to integrate and connect the transport of water vapor and heat from vegetation to the atmosphere and also with the possibility of studing the impact of external forcings to the system. We conclude from this study that there is a constant two-way feedback between the vegetation and the atmosphere; and that we observe this effect at different scales.

APPENDIX A – DESCRIPTION OF CLASS

In this Appendix we present a brief background of CLASS (Chemistry Land-surface Atmosphere Soil Slab).

CLASS is a 0-D model that uses the mixed-layer theory to represent the processes within the convective boundary layer (CBL). This layer develops from sunrise until sunset and it is in direct contact with the surface. During the day thermal plumes transport moisture and heat from the surface to the top of the CBL (~1km depth in the afternoon). The thermals mix the air with the downward transport of dry air entrained from the free troposphere until it is well mixed. Therein, it is considered that the potential temperature, the specific humidity and other atmospheric constituents remain constant with height. This is the main principle governing the processes in the CBL.

We can picture the CBL as a box wherein two main variables, temperature and humidity, are fluctuating due to the entrainment of warm and dry air at the top of the box (the troposphere) and the transport of heat and moisture at the bottom of the box (the surface). This last one controls strongly the variability in the temperature and humidity due to the turbulent processes that change during the day. Herein, to complete the study of the dynamics in the CBL we need to connect the atmosphere and the surface fluxes which are dependent on the vegetation and soil properties. We call this the coupled system or land-atmosphere system.

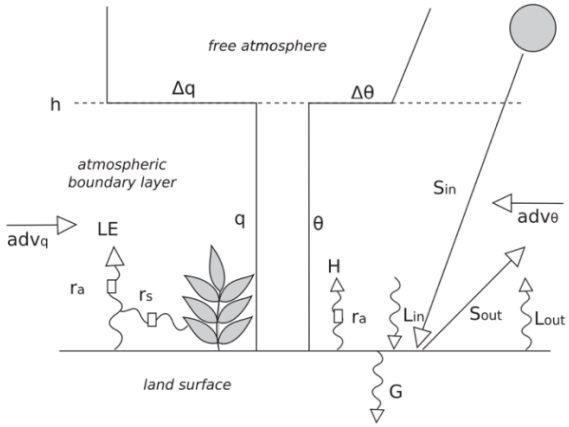

Figure A.1 Processes involved in the land-atmosphere system [23]

Figure A.1 illustrates the main processes and variables involved in the land-atmosphere system and that are modeled in CLASS. The net radiation (*Rn*) as an external forcing is defined by the incoming and outgoing shortwave (*Sin, Sout*) and longwave (*Lin, Lout*) radiation. This term defines the available energy and its partition into sensible heat (*H*), latent heat (*LE*) and ground (*G*) fluxes. The set of equations that CLASS uses for representing the surface fluxes is presented in the Appendix A.

In CLASS, LE is defined as the total evapotranspiration considering the fraction of water vapor that comes from vegetation, water sources and the soil. Another important term connected to LE is the stomatal resistance r_s. As explained in Chapter 1, it controls not only the rate of CO_2

assimilation but also the water vapor that is released to the atmosphere. A similar term r_{soil} is considered in the evaporation from soil to represent the rate capacity of water vapor released. We collected the data from the CloudRoots campaign, which has information at the surface level and the boundary layer to create a case study in CLASS that considers the interactions seen in Figure 2.3 and the evolution of the thermodynamic properties in this layer.

System of equations in CLASS

We present in this section the system of equations that CLASS includes to represent the evolution of the boundary layer growth, the potential temperature and moisture in this convective boundary layer. The complete derivation of the equations can be found in [14].

Equation (1) represents the evolution of the bulk potential temperature $<\theta>$ with time (the term bulk is used to express that the quantity is constant with height). It depends on the amount of heat that is transported from surface to the atmosphere as turbulent flux $(\overline{w'\theta'})_s$ and from the free troposphere as entrainment flux $(\overline{w'\theta'})_e$. h is the boundary layer height.
The advection term combines in a single term the wind and horizontal gradients of potential temperature, as shown in equation (2) Figure 2.2 shows the vertical profile of the potential temperature in the CBL.

$$\frac{\partial <\theta>}{\partial t} = \frac{(\overline{w'\theta'})_s - (\overline{w'\theta'})_e}{h} + \theta_{adv} \tag{1}$$

$$\theta_{adv} = -\left(U\frac{\partial \theta}{\partial x} + V\frac{\partial \theta}{\partial y}\right) \tag{2}$$

The evolution of the potential temperature jump at the boundary layer height $\Delta\theta_h$ (the difference in potential temperature between the CBL and the free troposphere) is defined in equation (2):

$$\frac{\partial \Delta\theta_h}{\partial t} = \gamma_\theta\left(\frac{\partial h}{\partial t} - w_s\right) - \frac{\partial <\theta>}{\partial t} \tag{3}$$

where γ_θ is the lapse rate of the potential temperature and w_s is the subsidence velocity.
Similar expressions are derived for the bulk specific humidity $<q>$:

$$\frac{\partial <q>}{\partial t} = \frac{(\overline{w'q'})_s - (\overline{w'q'})_e}{h} + q_{adv} \tag{4}$$

$$q_{adv} = -\left(U\frac{\partial q}{\partial x} + V\frac{\partial q}{\partial y}\right) \tag{5}$$

$$\frac{\partial \Delta q_h}{\partial t} = \gamma_q\left(\frac{\partial h}{\partial t} - w_s\right) - \frac{\partial <q>}{\partial t} \tag{6}$$

And finally, the growth evolution of the boundary layer height is defined as:

$$\frac{\partial h}{\partial t} = \frac{(\overline{w'\theta_v'})_e}{\Delta\theta_{vh}} + w_s \tag{5}$$

where $(\overline{w'\theta_v'})_e$ is the entrainment flux of the virtual potential temperature and $\Delta\theta_{vh}$ is the jump at boundary layer height of the virtual potential temperature.

Partition of net energy into the surface fluxes:

$$R_n = H + LE + G \tag{6}$$

$$H = \frac{\rho C_p}{r_a}(\theta_s - <\theta>) \tag{7}$$

$$LE_{tot} = LE_{veg} + LE_{liq} + LE_{soil} \tag{8}$$

$$LE_{veg} = \frac{\rho L_v}{r_a + r_s}(q_{sat}(T_s) - <q>) \tag{9}$$

$$LE_{liq} = \frac{\rho L_v}{r_a}(q_{sat}(T_s) - <q>) \tag{10}$$

$$LE_{soil} = \frac{\rho L_v}{r_a + r_{soil}}(q_{sat}(T_s) - <q>) \tag{11}$$

$$G = \lambda_s(T_{surface} - T_{soil}) \tag{12}$$

In (7), ρ is the air density, c_p is the specific heat capacity of air at constant pressure and θ_s is the potential temperature at surface. The aerodynamic resistance r_a represents the connection between the surface and the atmosphere because it is considered as a rate capacity to exchange heat and moisture between these two systems.

From the previous set of equations, L_v is the latent heat of vaporization, $q_{sat}(T_s)$ is the saturated specific humidity at surface temperature T_s and λ_s is the effective conductivity of heat. G is defined as the temperature gradient between the surface and a deeper soil layer.

Bibliography

1. de Boer, H.J., et al., *Climate forcing due to optimization of maximal leaf conductance in subtropical vegetation under rising CO2.* Proceedings of the National Academy of Sciences, 2011. **108**(10): p. 4041-4046.
2. Williams, I.N. and M.S. Torn, *Vegetation controls on surface heat flux partitioning, and land-atmosphere coupling.* Geophysical Research Letters, 2015. **42**(21): p. 9416-9424.
3. Moene, A.F. and J.C. Van Dam, *Transport in the atmosphere-vegetation-soil continuum*. 2014: Cambridge University Press.
4. LeMone, M.A. and W.T. Pennell, *The relationship of trade wind cumulus distribution to subcloud layer fluxes and structure.* Monthly Weather Review, 1976. **104**(5): p. 524-539.
5. Ronda, R., H. De Bruin, and A. Holtslag, *Representation of the canopy conductance in modeling the surface energy budget for low vegetation.* Journal of Applied Meteorology, 2001. **40**(8): p. 1431-1444.
6. van Heerwaarden, C.C. and J.V. Guerau de Arellano, *Relative humidity as an indicator for cloud formation over heterogeneous land surfaces.* Journal of the Atmospheric Sciences, 2008. **65**(10): p. 3263-3277.
7. Raupach, M., *Vegetation-atmosphere interaction and surface conductance at leaf, canopy and regional scales.* Agricultural and Forest Meteorology, 1995. **73**(3-4): p. 151-179.
8. Wolf, B., et al., *The SCALEX campaign: Scale-crossing land surface and boundary layer processes in the TERENO-preAlpine observatory.* Bulletin of the American Meteorological Society, 2017. **98**(6): p. 1217-1234.
9. Vico, G., et al., *Effects of stomatal delays on the economics of leaf gas exchange under intermittent light regimes.* New Phytologist, 2011. **192**(3): p. 640-652.
10. Vilà-Guerau de Arellano, J., et al., *Shallow cumulus rooted in photosynthesis.* Geophysical Research Letters, 2014. **41**(5): p. 1796-1802.
11. Horn, G., et al., *Cloud shading effects on characteristic boundary-layer length scales.* Boundary-Layer Meteorology, 2015. **157**(2): p. 237-263.
12. Pedruzo-Bagazgoitia, X., et al., *Direct and diffuse radiation in the shallow cumulus–vegetation system: Enhanced and decreased evapotranspiration regimes.* Journal of Hydrometeorology, 2017. **18**(6): p. 1731-1748.
13. Doutriaux-Boucher, M., et al., *Carbon dioxide induced stomatal closure increases radiative forcing via a rapid reduction in low cloud.* Geophysical Research Letters, 2009. **36**(2).
14. Vilà-Guerau de Arellano, J., et al., *Atmospheric boundary layer: Integrating air chemistry and land interactions*. 2015, Cambridge University Press, Cambridge, UK.
15. Langensiepen, M., et al., *Improving the stem heat balance method for determining sap-flow in wheat.* Agricultural and forest meteorology, 2014. **186**: p. 34-42.
16. Ney, P. and A. Graf, *High-resolution vertical profile measurements for carbon dioxide and water vapour concentrations within and above crop canopies.* Boundary-Layer Meteorology, 2018. **166**(3): p. 449-473.
17. Jakobi, J., et al., *Cosmic Ray Neutron Sensing for Simultaneous Soil Water Content and Biomass Quantification in Drought Conditions.* Water Resources Research, 2018. **54**(10): p. 7383-7402.
18. Rascher, U., et al., *Sun-induced fluorescence–a new probe of photosynthesis: First maps from the imaging spectrometer HyPlant.* Global change biology, 2015. **21**(12): p. 4673-4684.
19. Blay-Carreras, E., et al., *Role of the residual layer and large-scale subsidence on the development and evolution of the convective boundary layer.* Atmospheric Chemistry and Physics, 2014. **14**(9): p. 4515-4530.
20. Lin, Z., et al., *The different influence of the residual layer on the development of the summer convective boundary layer in two deserts in northwest China.* Theoretical and Applied Climatology, 2018. **131**(3-4): p. 877-888.
21. Bleam, W., *Chapter 2 - Chemical Hydrology*, in *Soil and Environmental Chemistry (Second Edition)*, W. Bleam, Editor. 2017, Academic Press. p. 39-85.
22. Ouwersloot, H., et al., *Characterization of a boreal convective boundary layer and its impact on atmospheric chemistry during HUMPPA-COPEC-2010.* Atmospheric Chemistry and Physics, 2012. **12**(19): p. 9335-9353.
23. van Heerwaarden, C.C., *Surface evaporation and water vapor transport in the convective boundary layer*. 2011.